Validation of a simple aerodynamic model capable to predict the interaction effects occuring between two generic wind propulsion systems

Bordogna, Giovanni; Keuning, Lex; Huijsmans, Rene; Fossati, Fabio Vittorio; Belloli, Marco

Publication date
2016

Document Version
Final published version

Published in
Proceedings of the12th International Conference on Hydrodynamics-ICHD 2016

VALIDATION OF A SIMPLE AERODYNAMIC MODEL CAPABLE TO PREDICT THE INTERACTION EFFECTS OCCURRING BETWEEN TWO GENERIC WIND PROPULSION SYSTEMS

G. Bordogna, J.A. Keuning and R.H.M. Huijsmans
Section of Ship Hydromechanics and Structures, Delft University of Technology
Mekelweg 2, 2628 CD Delft, The Netherlands
g.bordogna@tudelft.nl, j.a.keuning@tudelft.nl, r.h.m.huijsmans@tudelft.nl

F.V. Fossati and M. Belloli
Department of Mechanical Engineering, Politecnico di Milano
Via la Masa 1, 20156 Milan, Italy
marco.belloli@polimi.it

ABSTRACT: The research presented in this paper deals with the validation of a simple aerodynamic model that is capable of evaluating the aerodynamic interaction effects, i.e. downwash and wake, occurring between two generic wind-propulsion systems installed on the deck of a ship. Such model consists of the horseshoe vortex method modified with a semi-empirical formula to take into account the effects of viscosity, and it is able to deal with attached as well as detached flows. The results provided by the aerodynamic model were compared with results obtained by using more sophisticated tools: a CFD body force method and a standard RANS solver. Experimental validation was also carried out by means of dedicated wind-tunnel tests. It can be concluded that, despite of its simplicity, the aerodynamic model employed proved to have a good potential.

INTRODUCTION

Wind energy as an auxiliary form of propulsion for commercial ships has again become of interest as a possible response to volatile fuel prices and increasingly stringent environmental regulations as supported by a recent study published by the Lloyd's Register [1] in 2015. The same study however, underlines how a well-founded performance prediction, i.e. how much fuel can be expected to be saved given a certain weather condition, is a key prerequisite for the further development and for the uptake of this promising technology.

From an aerodynamics perspective, it appears that there is a sufficient number of information available regarding the performance of various wind-propulsion systems (e.g. Dynarig, Flettner rotor, rigid wing, etc.), meaning that the amount of lift and drag that each system is able to generate given a certain angle of attack (or spinning velocity for the rotor) can be promptly estimated. On the other hand, much fewer details are known regarding the performance of these systems when installed on the ship's deck. The reason of this difference is to be found in all the complex aerodynamic interaction effects that occur on board of the ship and that eventually have an impact on the amount of wind-generated thrust. Such effects are mainly of two types; the interaction effects occurring among the several wind propulsion systems mounted on the ship's deck and the interaction effects occurring between the wind-propulsion systems and the ship itself (hull, superstructure, cargo, etc.). Due to the complexity of these phenomena and the lack of simple methods to include them in the performance

prediction, they were often neglected although their impact on the overall performance of the ship was proven by studies such as [2].

The work herewith presented is the first step in the development of an aerodynamic model capable to predict the interaction effects occurring among generic wind-propulsion systems. The model will be eventually integrated into a computer program that will allow designers to quickly and accurately evaluate the performance of different wind-assisted ships. Keeping in mind the purpose of such a program, it was necessary to build a simple and quick-to-use model. A good candidate was identified in the model proposed by Roncin and Kobus [3], which comprises a version of the horseshoe vortex method modified to take into account the viscous effects. Apart its simplicity, the great advantage of this model is that use can be made of the information already available on the aerodynamic characteristics of single wind-propulsion systems, i.e. their lift and drag coefficients. With this information the velocity field (downwash and wake) around a certain wind-propulsion system can be calculated and eventually it can be used to compute the aerodynamic forces that a second nearby propulsor would generate.

In this paper the velocity field generated by a rigid Dynarig set at different angles of attack is used for the validation of the simple aerodynamic model proposed. First, the results of the modified horseshoe vortex method are compared with results obtained by using more sophisticated tools, i.e. a CFD body force method and a standard RANS solver. Then the results of the considered methods are compared with data acquired during dedicated wind-tunnel experiments.

TEST CASE

The wind-propulsion system considered for the test case is a rigid Dynarig with span of 1.3 m, chord length of 0.7 m and camber of 10% (see Fig. 1).

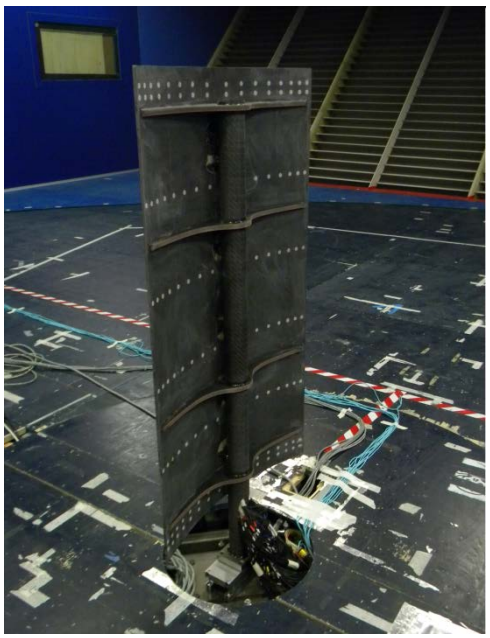

Figure 1- Dynarig used as test case

The Dynarig was mounted on a 1.5 m high mast with diameter of 0.07 m. The wind speed was set to 10 m/s leading to a Reynolds number $\mathrm{Re} = 4.7 \cdot 10^5$.

PRESENTATION OF THE NUMERICAL METHODS

Modified horseshoe vortex method

The modified horseshoe vortex method is composed by two independent parts: the inviscid and the viscous part. The inviscid part is based on the classic vortex theorems of Kelvin, Helmholtz and Biot-Savart by which the horseshoe vortex comprises one bound vortex and two semi-infinite vortices. The velocity induced by the horseshoe vortex is given in any point in space by the sum of the three vortex segments:

$$\mathbf{V} = \mathbf{V}_{AB} + \mathbf{V}_{A\infty} + \mathbf{V}_{B\infty} \tag{1}$$

and it is linearly dependent on the amount of circulation generated by the wind-propulsion system considered. The circulation is defined as:

$$\Gamma = \frac{\text{Lift}}{\left(span \cdot \rho_{air} \cdot V_{wind}\right)} \tag{2}$$

The viscous part comprises a semi-empirical formula proposed by Schlichting [4] to compute the wake downstream an element of known drag. The formula reads:

$$b = 1.14\left[C_D \cdot d_w \cdot x\right]^{p_1}$$
$$V_{(y)} = V_{wind} \cdot \left\{1 - 0.98\left[\frac{x}{C_D \cdot d_w}\right]^{p_2} \cdot \left[1 - \left(\frac{2 \cdot y}{b}\right)^{1.5}\right]^2\right\} \tag{3}$$

in which C_D is the drag coefficient, d_w is the width of the element, x is the distance downstream and p_1 and p_2 are tweaking factors ranging from -1 to 1.

RANS solver

The CFD software used in the present work was the *simpleFoam* solver of *OpenFOAM.* The simulation domain was divided into two regions, an outer region and a refinement box, in which the velocity field was sampled at various locations in space. The domain was discretised with about 1.1 million unstructured cells and the Dynarig's boundary layer refinement was made such that the values of y^+ ranged from 35 to 110 regardless the angle of attack considered. It should be pointed out that the mast and the yards of the Dynarig were not taken into account in the CFD model, just the planform was discretised.

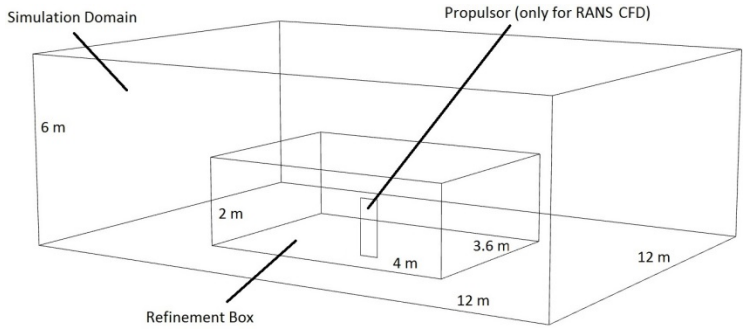

Figure 2- Simulation domain of the RANS solver and of the body force method

Initially, the $k-\omega$ STT turbulence model was chosen to solve the RANS equations, nevertheless the simulations failed to converge when the angle of attack was increased to 45° and to 90°. For this reason, it was decided to use the standard $k-\varepsilon$ model that, despite not being very suitable for such simulations, led to converged results. The convection term was interpolated with a first/second order scheme named *linearUpwind* in *OpenFOAM*.

Body force method

The body force method was implemented into the CFD software *OpenFOAM* and was based on the actuator line theory, by which a volumetric force can be input in the simulation domain. The RANS equations were then solved in the same manner of a standard CFD solver.

For each angle of attack, the lift and drag force were distributed in the simulation domain over a cylindrical volume that had the same span and diameter (chord length) of the Dynarig.

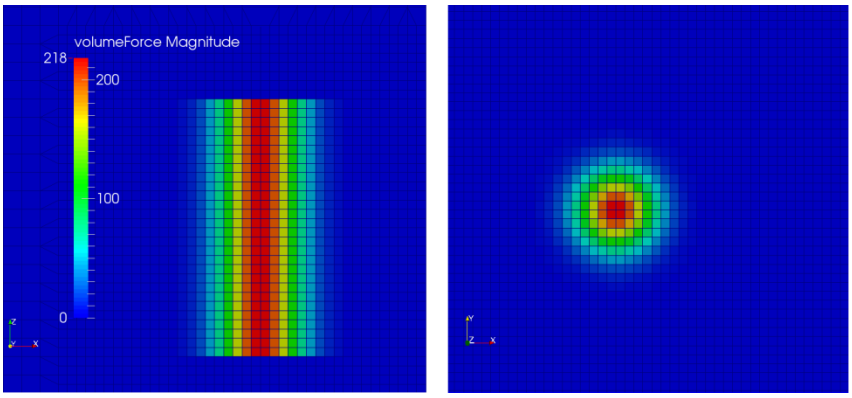

Figure 3- Volume force distribution: side view (left) and top view (right)

The domain, the mesh and the numerical methods were the same of those employed for the standard RANS solver with the exception that in this case converged solutions were also obtained when the $k-\omega$ STT turbulence model was used.

EXPERIMENT SETUP

The experiments were carried out in the boundary layer chamber of Politecnico di Milano wind tunnel. This chamber has a cross section of 13.8 m x 3.8 m and a length of 36 m. The Dynarig was mounted on a Ruag 192 scale at the centre of the turntable that was manually adjusted in order to change the angle of attack. Due to its mast, the Dynarig's planform was raised 0.20 m from the ground, meaning that it was entirely above the typical boundary layer height of the wind tunnel (0.15 m). The turbulence intensity of this chamber is about 2%.

The velocity field was sampled by using 4 Cobra probes mounted on a vertical bar connected to a toothed belt that, by activating an electric motor, could laterally move the probes to a maximum of 1.5 m left or right the centre of the Dynarig (see Fig. 4). The probes were located at 50 mm inwards from the top and bottom edge of the Dynarig's planform and equally spaced. The drag force and the X velocity component of the velocity field were aligned with the centreline of the wind tunnel while the lift force and the Y velocity component were perpendicular to the wind direction and had positive sign as shown in Fig.4.

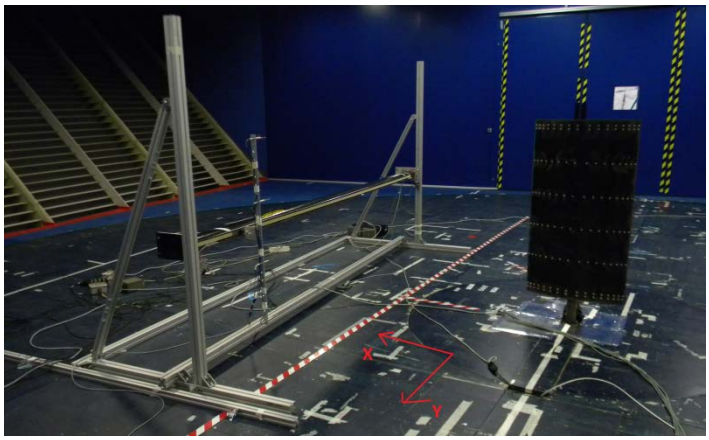

Figure 4- Dynarig with the setup to sample the velocity field

The velocity field was sampled for 3 different angles of attack; AoA=5°, AoA=45° and AoA=90°. For each angle of attack, 3 different longitudinal positions were tested, namely 1.5, 2.5 and 4 chord lengths downstream the Dynarig and, for each longitudinal position, the velocity field was measured at 25 transverse stations, one every 0.12 m. At every station a 60 second long measurement was taken.

RESULTS

The lift and drag coefficients of the Dynarig were measured for angles of attack ranging from 0° to 90°, while the velocity field was sampled only at angles of attack 5°, 45° and 90°. These angles of attack were chosen due to their relevance in order to validate the modified horseshoe vortex method. In fact, at AoA=5°, the Dynarig generates mainly lift ($L/D \approx 5$), at AoA=45° lift and drag have approximately the same magnitude, and at AoA=90° the Dynarig generates purely drag. The results obtained for angles of attack 5° and 90° were used to validate the inviscid and viscous parts of the aerodynamic model respectively, while the results of AoA=45° indicated the influence on the velocity field of the cross effects of lift on drag and likewise of drag on lift.

The RANS simulations were carried out for the same 3 angles of attack and the results are shown in Fig. 5. As expected the results compare well for AoA=5°, whereas when the angle of attack is increased to AoA=45° and AoA=90° the agreement between the CFD results and the experiments becomes poor. This is due to the well-known limitations of the RANS solvers, and in particular of the $k-\varepsilon$ turbulence model, in dealing with largely separated flows.

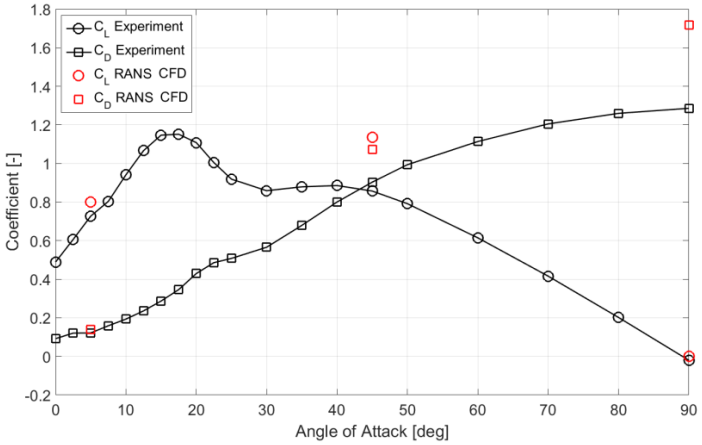

Figure 4- Dynarig lift and drag coefficient curves

The values of the lift and drag coefficients measured during the experiments were used in the modified horseshoe vortex method and in the body force method in order to generate the corresponding velocity fields. In all cases, in the experiments as well as in the numerical methods, the X and Y velocity components of the velocity field were sampled as described in the previous section at 4 different heights along the Dynarig's span and then averaged. Exception was made for the modified horseshoe vortex method in which the velocity field was sampled at only 1 height, namely at half span.

The results are herewith presented in terms of X velocity and Y velocity as fraction of the incoming flow speed. The first term indicates the reduction in longitudinal velocity (wake), while the second one indicates the change in flow direction (up/downwash).

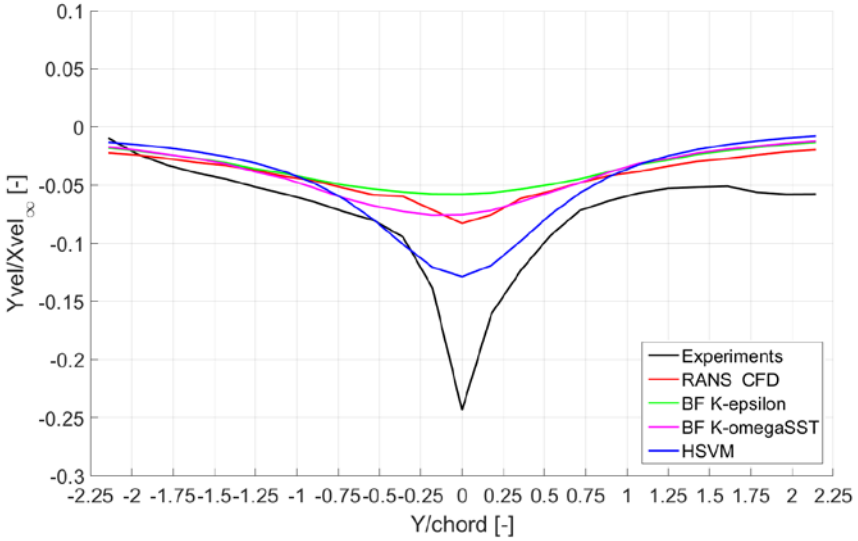

Figure 5- Y velocity: angle of attack 5°, distance 2.5 chord lengths downstream

In Fig. 5 the results relative to AoA=5° and a downstream distance of 2.5 chord lengths are shown. It can be seen that the experimental results indicate a very pronounced peak straight behind the Dynarig. The body force method, regardless the turbulence model employed, fails to predict any peak. The downwash is in fact smoothly distributed over all Y/chord values. The results obtained with the RANS solver do indicate a noticeable downwash increase at Y/chord=0, but it is still 75% smaller compared to the experimental data. The horseshoe vortex seems to be the numerical method that performs the best, although the difference with the experiments is still as large as 50%. Another discrepancy between the results computed and the experimental data is that the latter also indicates a small but noticeable downwash at positive Y/chord values that correspond to the area behind the low pressure side of the Dynarig.

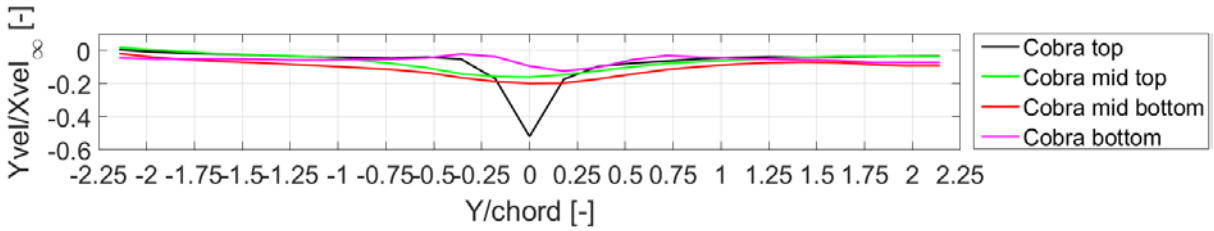

Figure 6- Sectional Y velocity: angle of attack 5°, distance 2.5 chord lengths downstream

Looking at the results of each individual Cobra probe (see Fig. 6), it can be seen that the main contribution to the downwash is given by the upper probe, meaning that the tip vortex shed at the upper edge of the Dynarig plays the most relevant role. The trend herewith analysed was also found for the other two longitudinal positions (1.5 and 4 chord lengths downstream).

The results relative to AoA=45° are important to understand the degree of interaction between the effects generated by lift and drag on the velocity field. In Fig. 7 and Fig 8 it can be seen that these effects are strongly related. Specifically, in Fig. 7, the results relative to the wake produced by the Dynarig at a distance equal to 4 chord lengths are shown. It is appreciable how the wake moved aside due to the lift-induced downwash.

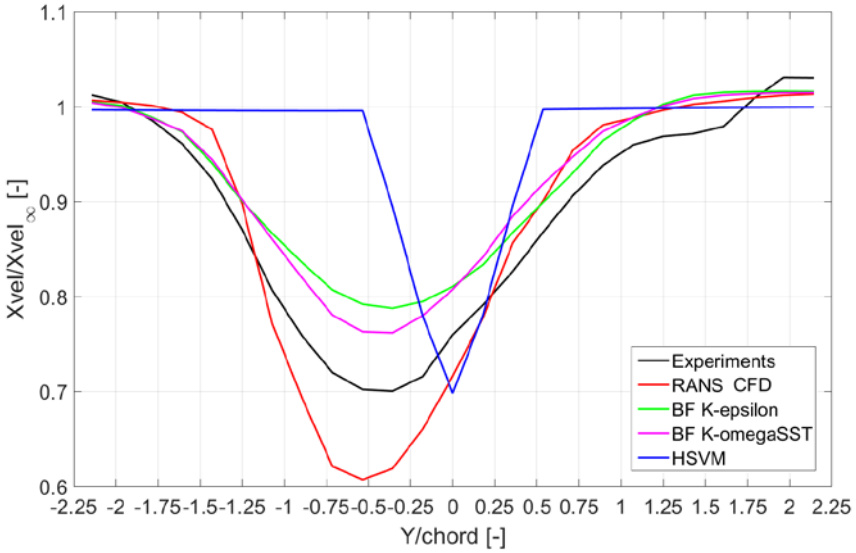

Figure 7- X velocity: angle of attack 45°, distance 4 chord lengths downstream

Similarly, in Fig. 8 it can be seen that for this angle of attack there is a substantial downwash as well as an upwash. The large downwash peak, noticeable at positive Y/chord values, is produced at the low-pressure side of the Dynarig. On the other hand, the upwash occurs in correspondence of the intrados at the trailing edge, where the flow separates due to the large angle of attack, and it turns towards the centreline of the Dynarig to reunite with the flow coming from the extrados.

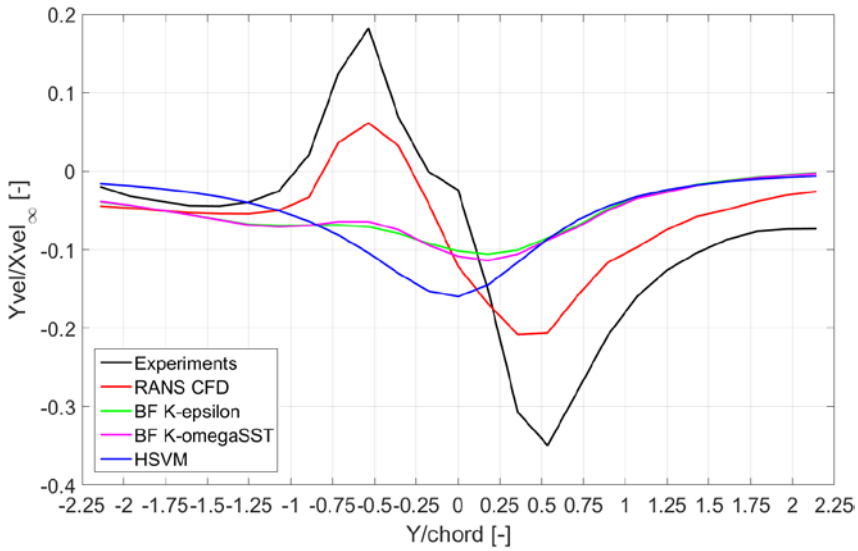

Figure 8- Y velocity: angle of attack 45°, distance 1.5 chord lengths downstream

Although to a different extent, the CFD methods are capable in dealing with the cross effects above described. On the contrary, the modified horseshoe vortex method, since its inviscid and viscous components work separately, is not capable to reproduce such effects.

Lastly, in Fig. 10 the results relative to AoA=90° and a longitudinal distance of 1.5 chord lengths downstream are given.

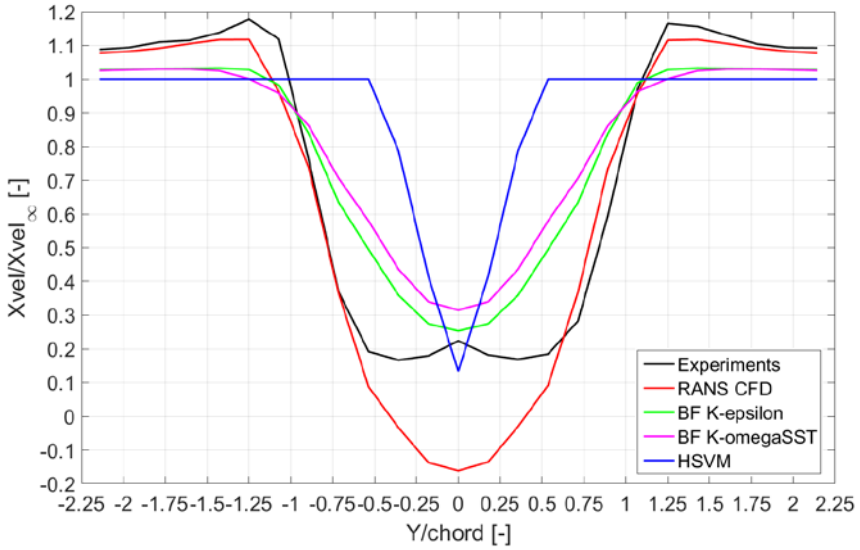

Figure 9- X velocity: angle of attack 90°, distance 1.5 chord lengths downstream

The experimental data show that at this angle of attack there is a substantial wake behind the Dynarig; the incoming flow velocity is in fact reduced by 80%. On the contrary, at the sides the flow is accelerated by up to 20%. The RANS solver gives a similar flow speedup but, at position Y/chord=0, it predicts an area of backflow that was not captured during the experiments. Oppositely, the body force method shows a comparable wake but a much reduced flow speedup compared to the experiments. Finally, the viscous part of the modified horseshoe vortex method proves to be able to correctly predict the magnitude of velocity reduction behind the Dynarig but the wake it is much narrower. Also, the flow velocity increase at the sides is completely neglected.

CONCLUSIONS

In this paper the capabilities of a modified version of the horseshoe vortex method to accurately compute the velocity field behind a given wind-propulsion system were compared with more sophisticated numerical tools as well as with experimental data obtained by means of dedicated wind tunnel tests. Among the numerical methods analysed, the horseshoe vortex method provided the most comparable results with the experimental data when looking at the downwash produced by the Dynarig at AoA=5°, although there was still a considerable difference. At AoA=90°, when the Dynarig generates only drag, the magnitude of the wake predicted by the viscous part of the horseshoe vortex method compares well with the experiments, however the shape of the wake it is much narrower. Also, the lateral velocity increase is completely neglected. Despite of its limitations, as far as the lift and drag cross effects can be neglected (i.e. at very small or very large angles of attack), the modified version of the horseshoe vortex method used in this work proved to give comparable or even better results than more sophisticated numerical methods. On the other hand, when such effects become of importance, i.e. when the lift and drag generated are of the same order of magnitude, the aerodynamic model proposed fails to provide satisfactory results.

To conclude it can be said that the modified version of the horseshoe vortex method used in the present work proved to have a good potential and it is a viable starting point in the development of a more elaborated aerodynamic model. Considering the outcome of the present study, the first modification that appears to be strictly necessary is the coupling of the inviscid and viscous components of the model.

REFERENCES

1. Argyros, D. (2015) Wind-powered shipping: a review of commercial, regulatory and technical factors affecting the uptake of wind-assisted propulsion, Lloyd's Register Marine
2. Fujiwara, T., Hearn, G.E., Kitamura, F. and Ueno, M. (2005) Sail-sail and sail-hull interaction effects of hybrid-sail assisted bulk carrier. *J. of Mar. Sci. Technol.* 10, 82-95
3. Roncin, K. and Kobus, J.M. (2004) Dynamic simulation of two sailing boats in match racing. *J. Sports Eng.* 7, 139-152
4. Schlichting, H. (1979*) Boundary layer theory*. Mc Graw-Hill, 7th edition, New York